Journal of Hazardous Materials 400 (2020) 123253

Contents lists available at ScienceDirect

Journal of Hazardous Materials

journal homepage: www.elsevier.com/locate/jhazmat

# Investigate the role of biofilm and water chemistry on lead deposition onto and release from polyethylene: An implication for potable water pipes

Tanvir Ahamed[a], Shawn P. Brown[b], Maryam Salehi[a,*]

[a] Department of Civil Engineering, The University of Memphis, Memphis, TN, USA
[b] Department of Biological Sciences, The University of Memphis, Memphis, TN, USA

## GRAPHICAL ABSTRACT

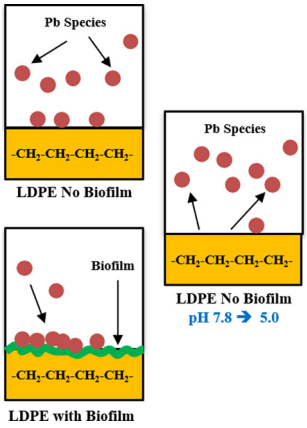


## ARTICLE INFO

Editor: R Teresa

*Keywords:*
Lead
Plastic pipes
Biofilm
Adsorption kinetics
Polyethylene

## ABSTRACT

In this study, the influence of biofilm presence and water chemistry conditions on lead (Pb) deposition onto low density polyethylene (LDPE) surface was examined. The results demonstrated that biofilm presence on LDPE surfaces strongly and significantly enhanced Pb uptake, with the 13-fold greater equilibrium Pb surface loading when biofilm was present (1602 μg/m$^2$) compared to the condition when it was absent (124 μg/m$^2$). The kinetics of Pb adsorption onto LDPE surface when biofilm was present is best described by Pseudo 2nd order kinetic model. Pb adsorption onto new LDPE surfaces was significantly reduced from 1101 μg/m$^2$ to 134 μg/m$^2$ with increased aqueous solution's ionic strength from $3 \times 10^{-6}$ M to 0.0072 M. The presence of chlorine residual (2 mg/L) significantly reduced Pb adsorption onto LDPE surfaces by possible oxidation of $Pb^{2+}$ to $Pb^{4+}$ species. The kinetics of Pb release from LDPE surfaces was investigated under static and dynamic conditions through immediate exposure of Pb accumulated LDPE pellets to the synthetic water at pH 5.0 and 7.8. The results demonstrated a greater Pb release (86 %) at pH 5.0 compared to the pH 7.8 (58 %). An enhanced Pb release into the contact water was found under dynamic conditions compared to static conditions.

* Corresponding author at: 3815 Central Avenue, 108 C Engineering Science Building, Memphis, TN, 38152, USA.
*E-mail address:* mssfndrn@memphis.edu (M. Salehi).

https://doi.org/10.1016/j.jhazmat.2020.123253
Received 24 March 2020; Received in revised form 16 June 2020; Accepted 17 June 2020
Available online 21 June 2020

## 1. Introduction

Lead (Pb) exposure through municipal tap water is a critical health concern nationally and globally. Lead in tap water remains an ongoing serious threat to public health, with recent large scale lead exposures occurring in Washington (DC), Flint (MI), and Newark (NJ) in the United States (Olson et al., 2017; Yang and Faust, 2019; Edwards et al., 2009). While the U.S. Environmental Protection Agency (US EPA) lead action level in drinking water is 15 μg/L, it was recommended by the American Association of Pediatrics that children do not expose to lead in drinking water at levels above 1 ug/L. (Council on Environmental Health, 2016) . Lead exposure can result in severe acute and chronic health impacts such as irreversible developmental and behavioral delays in children, hearing problems, renal dysfunction and delay in postnatal growth (Salehi et al., 2017; Edwards et al., 2009; Jain et al., 2005; DeSimone et al., 2020). Lead in tap water predominantly originates from corrosion of lead-bearing plumbing materials including lead service lines, brass valves and fittings, galvanized iron, lead-tin solder, and faucets (Boyd et al., 2008; Subramanian et al., 1995). A recent field investigation revealed Pb release (1 − 13 μg/L) into residential building tap water when the building plumbing is plastic (PEX-a) with Copper service lines (Salehi et al., 2019). These low levels of Pb in residential plumbing in the absence of lead component piping varied across plumbing fixtures. Lead likely originated from ball valves, brass barb tees, brass elbows, and faucets in this system (Salehi et al., 2018a; Huang et al., 2019a). Elfland et al. (2010) reported lead levels as high as 350 μg/L from the water fountains in a new building which the brass fittings were contributed to this lead contamination (Elfland et al., 2010).

The goal of increased sustainability coupled with the lower installation costs of plastic pipes has driven the increased usage of plastic pipes for building plumbing renovations and construction of new potable water systems. The global demand for plastic pipes has been estimated to be growing more than 4% per annum (Stewart, 2005). Plastic pipes are considered durable and easy to install, which further stimulates the demand. Moreover, the smooth plastic pipe surfaces are considered to be less susceptible to the accumulation of deposits (Rożej et al., 2015; Shakhsi-Niaei and Salehi Esfandarani, 2019). Additionally, polymer plastic pipes do not have corrosion problems like their metallic and concrete counterparts (Whelton and Nguyen, 2013). Building owners can receive LEED certification by the U.S. Green Building Council if they install plastic instead of copper piping (LEED for Homes Rating System, 2008). Crosslinked polyethylene (PEX) pipes are being installed in 75 % of new building construction and 54 % of renovations in the U.S., and high density polyethylene (HDPE) is used for water service connections (Kelley et al., 2014). Lead service lines, which are frequently found in the older buildings, are often connected to the recently renovated building plastic plumbing system. Thus, service line corrosion products can be released into the building plumbing and subsequently accumulate on the plastic pipes' inner walls. Our recent studies have demonstrated plastic plumbing pipes can play a major role in heavy metal accumulation by providing micro-resting sites where the presence of surface oxidized functional groups including > C-O < , > C = O, > COO can promote Pb species accumulation onto the low density polyethylene (LDPE) surface (Salehi et al., 2017, 2018b; Huang et al., 2019b). There has been extensive research conducted on plastic pollution within marine and fresh water environment which has demonstrated the influence of water chemistry conditions such as pH, ionic strength, ion competition dynamics, all of which directly influences metal adsorption onto the plastics (Holmes et al., 2014; Turner and Holmes, 2015; Santos-Echeandía et al., 2020). However, mechanistic understanding of how these parameters influence heavy metals accumulation onto the plastic drinking water plumbing is still lacking. Plastics are generally considered chemically inert materials with no inherent surface charge, but long term exposure to disinfectant residuals, surface precipitation of minerals scale, and biofilm accumulation could increase their susceptibility as a charged and porous media for heavy metal adsorption (Holmes et al., 2014). Further, plastic aging influences Pb uptake by LDPE pellets by forming and increasing the diversity of polar functional groups on the LDPE surface and by altering LDPE surface morphology (Salehi et al., 2018b). A recent study has shown that 10 h ozone aged LDPE pellets adsorbed up to 5 times more of heavy metals (Cu, Mn, Pb, and Zn) than new LDPE pellets (Huang et al., 2019b). A significant reduction was found in the Pb surface loadings on new and aged LDPE pellets when water pH is increased from 7.8–11 at a Pb concentration of 300 μg/L (Salehi et al., 2018b). Water chemistry fluctuations could result in detachment and dissolution of Pb corrosion products into tap water (Wang et al., 2010; Masters et al., 2016; Liu et al., 2009). The effect of disinfectant residuals on heavy metal release from metallic drinking water distribution pipes has been well studied (Zhang and Edwards, 2011; Rajasekharan et al., 2007; Switzer et al., 2006), but their influence on heavy metal fate in plastic plumbing materials has received much less scrutiny. Free chlorine residuals present in distribution systems could rapidly oxidize $Pb^{\circ}$ to $Pb^{2+}$ and subsequently to $Pb^{4+}$, which can aid in the precipitation of Pb in the form of α-$PbO_2$ (scrutinyite) and β-$PbO_2$ (plattnerite) as shown by Eq. 1 and 2 (Xie, 2010).

$$Pb + HOCl + H+ \rightarrow Pb2 + + Cl- + H2O \quad E^0_H = 1.47\,(V) \tag{1}$$

$$HOCl + Pb2 + + H2\,O \rightarrow PbO2 + Cl- + 3H+ \quad E^0_H = 1.48\,(V) \tag{2}$$

Microorganisms ubiquitously present in municipal water sources can colonize pipe surfaces and many of these can produce extracellular polymeric substances (EPS) which facilitates additional microbial adherence until it creates a biofilm that continues to grow and can even propagate thereby establishing new biofims (González-Rivas et al., 2018). Biofilms may adhere to the pipe surface initially by the weak van der Waals forces and hydrophobic effects. These biofilms can accumulate on pipe surfaces and critically influence the heavy metal fate and transport within the plastic plumbing (Niquette et al., 2000). Biofilms present on plastic surfaces improve heavy metal adsorption capacity by altering the surface charge, surface roughness, surface free energy, and electrostatic interactions (Lehtola et al., 2006; Rummel et al., 2017). Marine plastic pollution studies have confirmed the role of biofilms on increased heavy metal uptake by microplastics (Munier and Bendell, 2018). However, there is a knowledge gap in how biofilms influence contaminant fate in plastic plumbing materials. While research has been conducted on the interactive effects of biofilms on pipe corrosion (Rhoads et al., 2017; Vargas et al., 2014; Marsili et al., 2018), the mechanistic role of biofilms on heavy metal uptake by plastic pipes has been overlooked. Metal deposition onto plastic pipes is not necessarily a public health threat by itself but can become so when these deposited metals are released into the water. Heavy metals deposited onto the pipe surface could release to the water under certain chemical, water flow or microbiological conditions. The fluctuations of water chemistry from using blending or differently sourced water can result in heavy metal dissolution from scales into water. Heavy metals could be released from water distribution networks and plumbing materials into residential water due to chemical or biological oxidations or physical mechanisms (hydraulic turbulence) (Vasquez et al., 2006; Peng et al., 2012; Proctor et al., 2020). With increased demand and installation of plastic piping materials for potable water systems, additional research is essential to understand the drivers of heavy metals fate and transfer within these materials.

The research aims to examine the factors that influence $Pb^{2+}$ deposition onto and release from LDPE surfaces. The LDPE polymer in the form of pellets and films were used for this study as the model plastic due to its simple chemical structure to facilitate surface characterization, biofilm quantifications, and exclude the influence of plastic additives incorporated into the pipe chemical matrix. It is important to note that LDPE pipes are not used for drinking water piping in the U.S., but are used in Europe for different domestic and irrigation purposes

(Salehi et al., 2018b). The specific objectives were to (1) investigate the impact of biofilms on Pb deposition onto LDPE; (2) examine the impacts of water chemistry conditions on Pb deposition onto LDPE, and (3) determine the factors that influence Pb release from LDPE surfaces.

## 2. Experimental

### 2.1. Materials

Low density polyethylene (LDPE) pellets were purchased from Sigma Aldrich (St. Louis, MO, USA). These pellets had an average diameter of 4.2 mm, and an average mass of 26 mg. The Lead (Pb) ICP-MS standard (1000 mg/L) and sodium hypochlorite (NaOCl) were purchased from RICCA (Arlington, TX, USA) and Alfa Aesar Chemical Inc (Tewksbury, MA, USA) respectively. The LDPE plastic films were purchased from McMaster-Carr (Santa Fe Springs, CA, USA) and were cut into the square shape (0.5 cm × 0.5 cm) prior to experiments. Ultrapure Milli-Q™ (18MΩ*cm) treated water was used to conduct all the experiments in this study. In addition to the new LDPE pellets, the LDPE pellets aged according to the method described by Salehi et al. (2018) by purging ozone for 10 h were utilized for X-ray Photoelectron Spectroscopy (XPS) study and 7.5 h aged LDPE pellets were utilized for Pb release experiments (Salehi et al., 2018b). The phosphate-buffered saline (PBS) solution (10X) was purchased from Thermo Fisher Scientific Inc (Waltham, MA, USA). Rhodamine 6 G stain (excited at 504 nm) was bought from EMD Chemical Inc (Gibbstown, NJ, USA). The synthetic tap water is used for all metal exposure and release experiments. Its composition was adapted from literature (Huang et al., 2019b) and is shown in **Table SI-1**. More details regarding the materials used in this study are described in **SI-1**.

### 2.2. Biofilm growth and quantifications

In this study, initially, the biofilms were grown on new LDPE pellets for 32 days at 22 °C ( ± 2 °C) using the municipal tap water (Memphis, TN, USA). For this purpose, the LDPE pellets were placed into a glass flask connected to the drinking water fixture located in the Environmental lab. The water was drained from the outlet of the flask where it was covered by the plastic net to prevent the LDPE pellets from leaving this system (**Figure SI-1**). The municipal tap water relied on groundwater sources and provided by the local water utility. The chemical characteristics of finished water as reported by the local water utility are listed in **Table SI-2**. Following the literature, the biofilms were grown on the pellets using a water flow of 0.35 L/min for 12 h and stagnation for in 12 h (Fish et al., 2015). An automated controlled solenoid valve was installed to open and close the valve to have the designated water flow and stagnation periods. During the biofilm growth process, total chlorine residual, pH, and temperature were monitored weekly. The average total chlorine and water pH were 1.1 mg/L ( ± 0.05) and 7.3 ( ± 0.10), respectively.

For visualization and quantification purposes, biofilms were grown on LDPE film (0.5 cm × 0.5 cm squares). In this process, the LDPE films underwent biofilm growth for 15, 30, 45, 60 and 90 days and these were removed from the flask at these timepoints. To quantify the surface area covered by biofilm, LDPE films were stained with 5 µL of rhodamine 6 G for 3 min and rinsed with a PBS buffer solution (Ohsumi et al., 2015; Richter-Heitmann et al., 2016). Because rhodamine 6 G binds strongly to negatively charged nucleic acids and proteins that are major components of biofilms, this allows fine-scale fluorescent imaging of biofilms (Priester et al., 2007). Images were taken on nine squares (16 mm × 16 mm) for each film using Olympus BX43 F (100 W Mercury Lamp Fluorescence Illuminator, 10X–40X magnification, 400 − 525 nm wavelength) equipped with an Olympus DP73 high-performance digital color camera and fluorescent light source. Images were taken by following a line from the center to the outer edge of each film. Image processing was implemented using MATLAB programming (Matlab™ vers. 9.4, The Mathworks, Inc) to obtain the binary images and calculate the percentage of area covered by biofilm.

To quantify biofilm accumulated onto the LDPE film surfaces, ten LDPE square films were placed in a 15 mL centrifuge tube containing 3 mL of PBS buffer solution (2X) on a shaker (250 rpm, 15 min) to remove the loosely adherent cells from the plastic surface. After that, the films were subjected to sonication using a sonication probe (output frequency 20 kHz, power 50 W, volts 24 V DC, current 3.75A max) for 5 min. The plastic tubes containing the films were cooled (4 ºC) during sonication steps to prevent the heat damage to the microbial cells. The PBS solutions were centrifuged (Eppendorf MiniSpin Plus 5453) at 4000 rpm for 5 min. Then, 5 µL of rhodamine 6 G stain was added to the sample and stained for 5 min. After that, 10 µL of each sample was pipetted onto a hemocytometer (Hausser Scientific Bright-Line™) and quantified using a rhodamine light cube. Respective cell numbers were calculated to present as cell densities per unit surface area of films (cells per $cm^2$). Three replicates were examined at each period, according to the method mentioned. Control experiments were conducted by taking the images of the stained film surface before and after the biofilm separation process to validate the effectiveness of the biofilm separation method (**SI-3**).

### 2.3. Kinetic experiments: five-day Pb exposure

New and aged LDPE pellets were conditioned following Salehi et al., 2018 (Salehi et al., 2018b) to exclude the influence of residual organics **(SI-2)**. The five-day Pb exposure experiments were conducted at pH 7.8 for new and aged LDPE pellets and pellets with biofilm. In these experiments, synthetic tap water was used. The surface area to volume ratio for the pellets was selected as 0.85 $cm^2$/mL similar to Salehi et al., 2018 (Salehi et al., 2018b). The Pb uptake by LDPE pellets was investigated after 2, 6, 12, 24, 48 h, and five days of exposure to the aqueous Pb solution ($[Pb]_t$ = 300 µg/L). Although a wide range of Pb concentration in potable water was reported in the literature (15 µg/L to 18,800 µg/L) DeSimone et al., 2020, but those extreme cases may rarely occur, so in this study a value which is 20 times greater than USEPA action level (15 µg/L) is selected. Furthermore, selecting this Pb concentration enabled the authors to compare their results with recent relevant published works (Salehi et al., 2018b; Huang et al., 2019c). During the experiments, three replicates (50 mL PTFE bottles) were removed at each time interval. To quantify Pb adsorbed by LDPE, the pellets were removed from the water and acidified with 2% $HNO_3$ for 24 h (Salehi et al., 2017, 2018b; Huang et al., 2019b, 2017; Huang et al., 2019d). Control experiments were conducted to quantify Pb on LDPE pellets that were colonized by biofilms but were not exposed to metal (Pb) solution. The influence of total chlorine residual on Pb deposition onto LDPE pellets was investigated by adjusting an initial total chlorine concentration of 2.0 ± 0.1 mg/L in an aqueous Pb solution of 300 µg/L and conducting the described kinetic experiment at pH 7.8.

### 2.4. Pb adsorption kinetic modeling

The kinetics of $Pb^{2+}$ uptake by LDPE pellets was studied using the Pseudo 1st order and 2nd order kinetic models. The $Pb^{2+}$ uptake by new LDPE pellets was considered as a mass transfer process, as the $Pb^{2+}$ species only transferred from the bulk solution to the plastic surface and no chemical reactions occurred. The Pseudo 1st order rate constant was determined using Eqs. (3–5): (Ho and McKay, 1999)

$$\frac{dq}{dt} = -K_1(q - q_{eq}) \tag{3}$$

$$q = q_{eq}(1 - e^{-K_1 t}) \tag{4}$$

$$t_{\frac{1}{2}} = \frac{ln2}{K_1} \tag{5}$$

Where q is the amount of Pb surface loading on LDPE (μg/m$^2$) at any given time t (hr), $q_{eq}$ is the amount of Pb surface loading on LDPE (μg/m$^2$) at equilibrium. The slope of the straight-line plot of ln($q_{eq}$-q) against t was used to calculate the Pseudo 1st order reaction rate constant for adsorption $K_1$ ($h^{-1}$). The $q_{eq}$ is approximated by taking the average of the last two concentrations in the exposure periods. The half-life (t ½) represents the time required for a polymer to uptake half of equilibrium Pb surface loading and calculated using Eq. 5. The Pseudo 2nd order kinetic model (Eq. 6–8) is generally applied when chemical reactions or association controls the adsorption process (Ho and McKay, 1999). Where q is the amount of Pb surface loading on LDPE (μg/m$^2$) at any given time t (hr), $q_{eq}$ is the amount of Pb surface loading on LDPE (μg/m$^2$) at equilibrium and h, is the initial adsorption rate at t→0. The Pseudo 2nd order reaction rate constant, $K_2$ and $q_{eq}$ values can be determined from the slope and intercept of the straight-line plot of t/q versus t. Both adsorption rate constants $K_1$ and $K_2$ are the time scaling factor, the value of which describes how fast the system reaches the equilibria. In this study, the distribution ratio (D) shows the Pb distribution between the LDPE surface and aqueous solution. The equation for the distribution ratio is shown in Eq. 9.

$$\frac{dq}{dt} = K_2(q_{eq} - q)^2 \tag{6}$$

$$\frac{t}{q} = \frac{1}{h} + \frac{t}{q_{eq}} \tag{7}$$

$$h = K_2 {q_{eq}}^2 \tag{8}$$

$$D(mm) = \frac{Pb\ Surface\ loading\ (\frac{\mu g}{m^2})}{Pb\ floc\ left\ in\ solution\ (\frac{\mu g}{L})} \tag{9}$$

### 2.5. Chlorine decay experiments

The kinetics of chlorine decay in an aqueous solution containing new LDPE pellets was examined in the presence and absence of $Pb^{2+}$ species ($[Pb]_t$ = 300 μg/L) through five days of exposure. The experiments were conducted at room temperature at pH 7.8, with an initial total chlorine concentration of 2.0 ± 0.1 mg/L. Total chlorine concentration was measured after 2, 6, 12, 24, 48 h, and five days of exposure periods. All the experimental total chlorine concentrations data were fitted into a 1st order chlorine decay model (Zhang et al., 2017).

### 2.6. Pb release experiments from LDPE surface

Before conducting the Pb release experiments, both new and aged LDPE pellets were exposed to a $Pb^{2+}$ solution ($[Pb]_t$ = 300 μg/L) for five days at pH 7.8. The pellets, which were aged for 7.5 h according to the method described by Salehi et al., 2018, (Salehi et al., 2018b) were used for release investigations. Twenty pellets were placed in 13 mL of solution in PTFE bottles to have a surface to volume ratio of 0.85 cm$^2$/mL. The Pb concentrations in aqueous solution and their loadings onto the plastic pellets were analyzed for three replicates at each time interval. After five days of Pb accumulation, the pellets were immediately exposed to the synthetic water at pH 5.0 under both stagnant and dynamic conditions, and at pH 7.8 under dynamic condition. Then the Pb release from pellets into the synthetic water was investigated by quantification of Pb in the contact water after 5 min, 2, 6, 12, 24, 48 h and five days exposure periods. Furthermore, to quantify the Pb left on the pellets, they were removed from the aqueous solution and acidified with 2% $HNO_3$ for 24 h.

### 2.7. X-ray photoelectron spectroscopy (XPS)

The X-ray photoelectron spectroscopy (XPS) was conducted to examine Pb oxidation due to the exposure to chlorine residuals. The 10 h ozone aged LDPE films were used for this XPS analysis to enhance the Pb accumulation onto the LDPE surface and improve its detection by XPS spectroscopy (Salehi et al., 2018b). These aged LDPE films were exposed $[Pb]_t$ = 10 mg/L and total chlorine concentrations 10 mg/L at pH 7.8, for 48 h and room temperature. The reason for increasing the Pb concentration at this experiment is related to the limitations involved in the X-ray photo electron spectroscopy (XPS). The preliminary tests revealed difficulties in identification the Pb oxidation states even at the Pb concentration of 5000 μg/L. The XPS spectroscopy was performed using a Thermo Scientific spectrometer XPS equipped with a monochromatic Al Kα radiation (hυ = 1486.6 eV). More details are described in **SI-4**.

### 2.8. Water quality analysis

Water pH was measured using a Fisherbrand™ accumet™ XL600 pH Meter. Pocket Colorimeter™ II, Chlorine was used to measure the total chlorine residual (detection limit 0.01 mg/L). Total Pb concentration in water was quantified using the Atomic Absorption spectrometer (AA400, HGA 900 Graphite Furnace). The instrument was calibrated using seven standards (0 μg/L, 5 μg/L, 50 μg/L, 100 μg/L, 150 μg/L, 200 μg/L, 300 μg/L). The limit of detection (LOD) was 2 μg/L (AAS). All standard curves had a coefficient of determination in the range of 0.95 to 0.99.

### 2.9. Statistical analysis

SPSS 26 was used to perform statistical analysis. The correlation between Pb uptake by LDPE pellets with a total chlorine residual was investigated by Pearson correlation at a 95 % confidence interval. Multiple regression models and Student t-tests were performed to identify the significant difference of Pb surface loading of different experiments. Statistical significance was assumed when adjusted *p*-value < 0.05.

## 3. Results and discussion

### 3.1. Influence of biofilm on Pb uptake by new LDPE

#### 3.1.1. Biofilm quantification

Fluorescence microscopy of the stained LDPE films revealed increased biofilm surface coverage over time, as shown in Fig. 1. The percentage of the surface area covered by biofilms has been calculated by dividing the number of white pixels to the total number of pixels for each binary image (Lewandowski et al., 1999; Yang et al., 2000; Salehi and Johari, 2011). As **Figure SI-2** demonstrates the percentage of the plastic surface area covered by biofilm increased exponentially (*Adj.* $R^2$ = *0.93,* $p < 0.05$) from 5.5 % after 15 days to 54 % after 90 days biofilm growth process. The solid-liquid interface between the film surface and aqueous medium may provide a proper environment for the further attachment and evolution of microorganisms. The initial microorganisms that bind can change LDPE surface properties so that additional cells can adhere via cell-to-cell association which may increase the stability of the biofilm community (González-Rivas et al., 2018; Rummel et al., 2017). Using the biofilm separation and quantification processes described in section 2.2 the number of cells per unit area of LDPE films was estimated as 76 ± 15 cells/ cm$^2$ after 15 days of the biofilm growth process which was increased to 650 ± 55 cell/ cm$^2$ after 90 days ($T = 8.16$, $F = 66.64$, *Adj.* $R^2 = 0.96$, $p = 0.004$). As it was demonstrated in **Figure SI-3**, the average number of cells per unit surface area of LDPE films follows an incremental order. To validate the efficiency of the biofilm separation process, the described image analysis approach was conducted for fluorescent images captured from five different stained LDPE films before and after the biofilm separation process (**SI-3**). The results revealed that on average, 70 % ± 6% biofilm

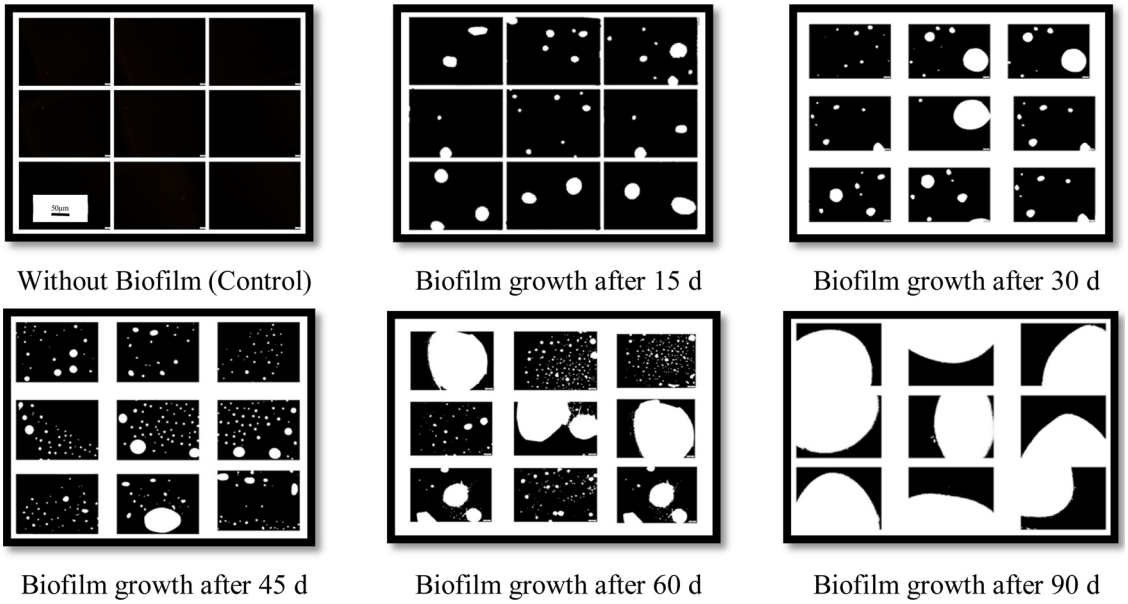


**Fig. 1.** Binary images showing biofilm-covered regions on the LDPE film surface.

surface coverage was separated (**Figure SI-4**). Both approaches were applied to quantify the biofilm surface loadings onto the LDPE films confirmed the increased biofilm growth over time.

### 3.1.2. *The influence of biofilm on Pb deposition onto LDPE*

The biofilms developed after 32 days onto the new LDPE pellets strongly and significantly ($T_{stat}$ = *-12.08,* $T_{crit}$ = *2.77,* $p$ = *0.0003*) enhanced the $Pb^{2+}$ adsorption during the 5-day exposure period (Fig. 2). At the equilibrium, the Pb surface loading on LDPE pellets with the biofilm (1602 μg/$m^2$) was more than 13-fold greater than the new LDPE with no biofilm (124 μg/$m^2$). While the LDPE surface with biofilm achieved 62.5 % of its surface loading equilibrium during the first 2 h of exposure, the LDPE with no biofilm obtained only 36 %. The Pb adsorption onto LDPE with biofilm increased during the 5-day exposure period, however for the LDPE with no biofilm, Pb surface loading reached equilibrium within 6 h. The distribution ratio (D) of 16.6 and 0.5 for LDPE with biofilm and no biofilm, respectively demonstrated the higher affinity of $Pb^{2+}$ species toward the plastic surface covered by biofilm compared to the condition where biofilm was absent. The biofilm accumulation onto LDPE has promoted the availability of surface sites for Pb deposition (Yee and Fein, 2002). Microbial cell walls contain numerous anionic functional groups (−COOH and $P-O_3^{2-}$), which may facilitate the adsorption of $Pb^{2+}$ complexes onto the cell surface (Fein et al., 1997).The extracellular polymeric substances (EPS) are a major component of biofilms are composed of several natural polymers (polysaccharides, proteins, lipids, and nucleic acids) with negatively charged functional groups like hydroxyl ($OH^-$) and sulfate ($SO_4^{2-}$) which may enhance the electrostatic attraction of $Pb^{2+}$ species toward the plastic surface. Other cellular processes like bioaccumulation (Muhammad et al., 1998), biotransformation, and passive processes like adsorption onto microbial cells, may also impact the $Pb^{2+}$ uptake (Feder et al., 2015). The experimental and calculated $q_{eq}$ values, Pseudo 1st order and 2nd order rate constants, half-life (t ½), distribution ratio (D), and coefficient of determinations ($R^2$) are summarized in Table 1. Using the Pseudo 1st order kinetic model, the equilibrium rate constants were determined as 0.0152 ($h^{-1}$) and 0.0388 ($h^{-1}$) for LDPE with biofilm and no biofilm, respectively. Thus, LDPE with no biofilm attained the equilibrium surface loading in a shorter time than LDPE with biofilm. These results indicate that the adsorption of $Pb^{2+}$ onto the LDPE with biofilm follows the Pseudo 2nd order kinetic model, as the chemical association was the potential rate-controlling factor. This finding agrees with the other studies which reported the Pseudo 2nd order kinetic model for biosorption of $Pb^{2+}$ ion from aqueous solution by biofilm biomass; however no one investigated $Pb^{2+}$ adsorption onto plastics surface in presence of microbial cells (Suguna and Siva Kumar, 2013; Olu-Owolabi et al., 2012; Javanbakht et al., 2011).

Following an increased LDPE film surface coverage by the biofilm, it

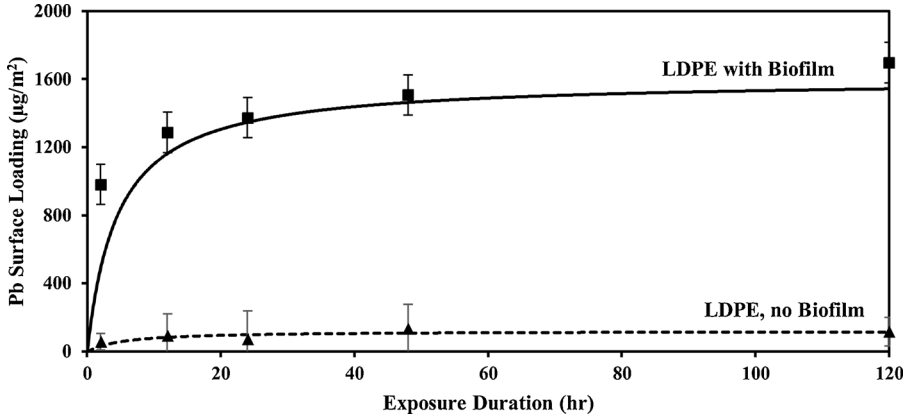


**Fig. 2.** The experimental results (Mean ± std) and Pseudo 2nd order model for Pb surface loading (μg/$m^2$) on LDPE/no biofilm and LDPE/biofilm overtime at pH 7.8.

**Table 1**
The parameters for Pseudo 1st order and 2nd order kinetics models.

| LDPE | Pseudo 1st order model | | | Pseudo 2nd order model | | | | Distribution Ratio (mm) |
|---|---|---|---|---|---|---|---|---|
| | K ($h^{-1}$) | $R^2$ | $t_{½}$ (h) | $q_{eq}$, Exp (μg/$m^2$) | K ($m^2$ $μg^{-1}$ $h^{-1}$) | $R^2$ | $q_{eq}$, Cal (μg/$m^2$) | |
| No Biofilm | 0.0152 | 0.89 | 45.40 | 124 | 0.0016 | 0.97 | 119 | 0.50 |
| With Biofilm | 0.0388 | 0.99 | 17.80 | 1602 | 0.0001 | 0.99 | 1667 | 16.65 |

was expected to have an increased order of Pb uptake by these films. Despite this expectation, conducting the 48 h $Pb^{2+}$ adsorption experiments using the LDPE films that undergone the biofilm growth process for 15 d, 30 d, 45 d, 60 d and 90 days have not revealed an ascending Pb surface loading order (**Figure SI-5**). The reason behind this may be the removal of individual cells or small groups of cells from the surface of the biofilm as the result of shear forces exerted by mixing the solution during the metal exposure experiment. This can also suggest that the LDPE films adsorbed $Pb^{2+}$ and with biofilm growth, this surface adhered Pb was removed by the bacteria for bio-sequestration, therefore; when cells were removed, this Pb consequently went to the solution.

### 3.2. Influence of water chemistry on Pb deposition onto new and aged LDPE

#### 3.2.1. Pb speciation in synthetic and DI water

As Fig. 3 demonstrates $Pb^{2+}$ ions form a variety of complexes with several anions ($OH^-$, $SO_4^{2-}$, $NO_3^-$, $Cl^-$, $HPO_4^{2-}$, $HCO_3^-$, $SiO_3^{2-}$) present in the synthetic drinking water. In this system, both $Pb(OH)_2$ and $PbCO_3$ were precipitated. However, they only create the hydroxyl complexes $(Pb(OH)^+$, $Pb(OH)_{2\ (aq)}$, $Pb(OH)_2$ (s), $Pb(OH)_3^-$ and $Pb(OH)_4^{2-})$ in the DI water (Salehi et al., 2018b). The $Pb^{2+}$ speciation in synthetic water was determined through solving $Pb^{2+}$ complexation and solubility equations (**Table SI-3)**. For the initial $Pb^{2+}$ concentration of 300 μg/L in synthetic water at pH 7.8, 20 % and 47 % of $[Pb]_t$ were precipitated as $[Pb(OH)_2](s)$ and $[PbCO_3](s)$ respectively, however, in DI water, 93.7 % of $[Pb]_t$ was precipitated as $[Pb(OH)_2](s)$ and no $[PbCO_3](s)$ was formed.

#### 3.2.2. Effect of ion's competition on $Pb^{2+}$ deposition onto new and aged LDPE

Our results (Fig. 4) demonstrated a significantly lower $Pb^{2+}$ uptake by both new and aged LDPE pellets in synthetic drinking water compared to their $Pb^{2+}$ uptake as reported by Salehi et al., (2018) in Ultrapure Millipore treated water under similar conditions (pH = 7.8, $[Pb^{2+}]_t$ = 300 μg/L). This lower Pb uptake by LDPE pellets could be described in terms of the difference in the ionic strength of synthetic drinking water (0.0072 M) and DI water ($3\times10^{-6}$ M). Additional ions present in the synthetic water may have competed with Pb species to occupy the LDPE available surface sites and resulted in the reduced Pb surface loading on LDPE pellets (Boudrahem et al., 2011). Surrounding the LDPE adsorption sites with counter ions present in synthetic water reduces their electrostatic attractions toward the Pb species existed in the aqueous environment (Vilar et al., 2007; Unuabonah et al., 2008). Furthermore, the solutions great ionic strength reduces the activity coefficient of $Pb^{2+}$ species, and limit their transfer to the LDPE surface (Wu et al., 2011). The lower $Pb^{2+}$ surface loading on new and aged LDPE pellets in synthetic water could be attributed to the competition of cations: $K^+$, $Ca^{2+}$, $Na^+$, $Mg^{2+}$, $Al^{3+}$, and co-anions: $Cl^-$, $SO_4^{2-}$, $HPO_4^{2-}$, $CO_3^{2-}$, $NO_3^-$ with $Pb^{2+}$ for electrostatic binding to the LDPE surface (Inglezakis et al., 2005). Consequently, $Pb^{2+}$ species adsorption become more competitive, in which different ions compete for a limited number of metal-binding sites on the LDPE surface. The degree of inhibition on Pb adsorption by available inorganic ions followed the sequence: $K^+ < Na^+ < Mg^{2+} < Ca^{2+} < Al^{3+}$. $Na^+$, $K^+$, $Mg^{2+}$and $Ca^{2+}$ inhibited adsorption because they outcompeted Pb ions for adsorption sites this decreasing the activity of Pb ions (Liu et al., 2013). As monovalent cations (i.e. $Na^+$ and $K^+$) are bound by ionic attraction, they do not compete directly with Pb ions to the binding sites onto the LDPE surface and therefore have less influence on the adsorption. Pb adsorption is influenced by the presence of anions following the order, $Cl^- > SO_4^{2-} > NO_3^-$ (Inglezakis et al., 2005). The negative effect of $Cl^-$, $SO_4^{2-}$, $HPO_4^{2-}$on Pb adsorption may be as a result of metal anion complexing since $Pb^{2+}$ forms some soluble complexes with the anions.

### 3.3. The influence of chlorine residuals on Pb deposition onto the LDPE surface

#### 3.3.1. The influence of chlorine residuals on the kinetics of Pb deposition onto new LDPE

The presence of chlorine residuals reduced $Pb^{2+}$ adsorption onto the new LDPE surface during the entire exposure period ($T_{stat}$ = *11.50*, $T_{crit}$ = *2.57*, $p$ = *0.0003*). When no chlorine residual was present, the equilibrium Pb surface loading on LDPE pellets (135 μg/$m^2$) was significantly greater than the condition that chlorine residuals were present (95 μg/$m^2$). Both Pseudo 1st and 2nd order kinetic models were fitted into the experimental data to obtain a better understanding of chlorine residual impact on Pb adsorption mechanisms. The graphical

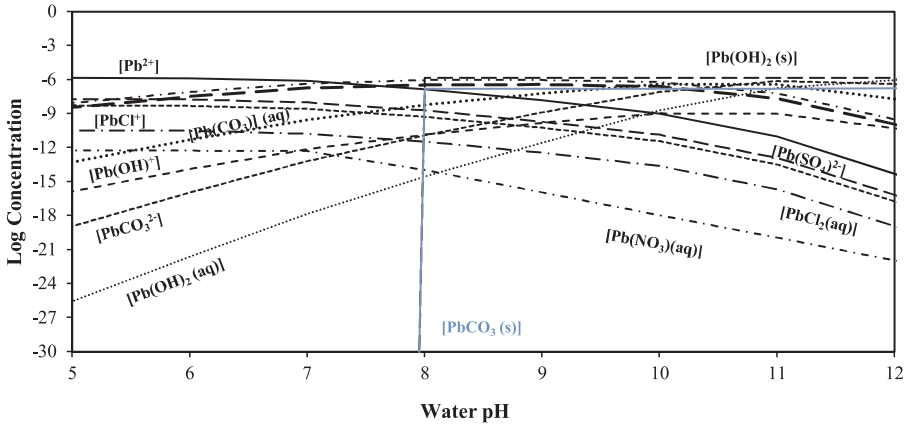


**Fig. 3.** Log concentrations for $Pb^{2+}$ species versus the water pH, $[Pb]_t$ = 300 μg/L.

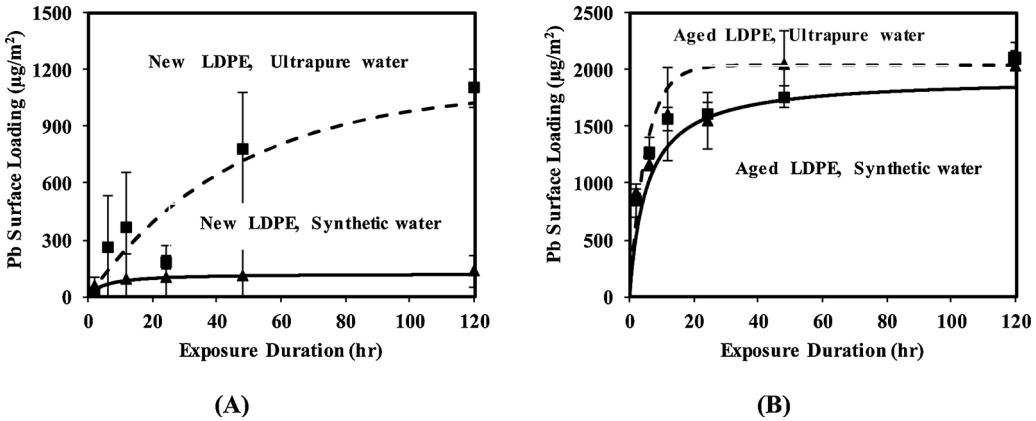


**Fig. 4.** Pb surface loading on (A) new LDPE and (B) aged LDPE in DI water and synthetic water at pH 7.8.

**Table 2**
The influence of chlorine residuals on the kinetics of Pb adsorption onto new LDPE.

| LDPE | Pseudo 1st order model | | | Pseudo 2nd order model | | | |
|---|---|---|---|---|---|---|---|
| | K ($h^{-1}$) | $R^2$ | $t_{½}$ (h) | $q_{eq,}$ Exp (µg/$m^2$) | K ($m^2$ µ$g^{-1}$ $h^{-1}$) | $R^2$ | $q_{eq,}$ Cal (µg/$m^2$) |
| No chlorine residuals | 0.039 | 0.99 | 18 | 124.9 | 0.00040 | 0.97 | 135.4 |
| With chlorine residuals | 0.036 | 0.99 | 19.25 | 98.5 | 0.00085 | 0.99 | 119.1 |

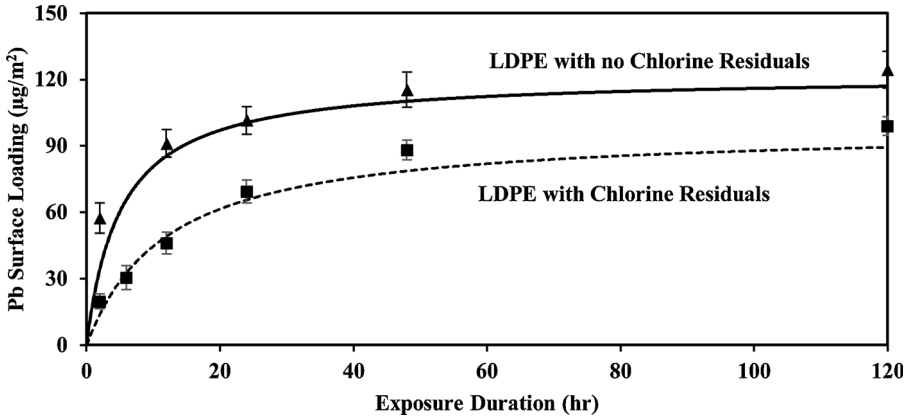


**Fig. 5.** Pb surface loading on LDPE with presence and absence of chlorine residuals.

demonstration of the Pseudo 1st order kinetic model and the kinetic rate constants are shown in Table 2 and Fig. 5, respectively. When no chlorine residuals were in the system, LDPE reached the equilibrium surface loading in a shorter time compared to the condition when the chlorine residuals were present. The chlorine decay was investigated in the synthetic water containing LDPE pellets in the presence and absence of $Pb^{2+}$, using 1st order chlorine decay model during the five day exposure period. (Powell et al., 2000a, b), No significant difference was found in the chlorine decay behavior due to the Pb presence in the aqueous solution ($p$-value > 0.05). That might be due to the significantly lower concentration of $Pb^{2+}$ (300 µg/L) compared to the total chlorine residuals (2 mg/L). Thus, the formation of possible chloro-complexes of Pb like, $PbCl^+$, $PbCl_2$, $PbCl_3^-$ and $PbCl_4^{2-}$ has not influenced the decay pattern. A negative correlation (-0.906) was found between Pb surface loading and total chlorine residual ($p$-value < 0.05) suggesting the impact of chlorine residual in preventing the Pb species from adsorption onto the LDPE surface (**Figure SI-6**).

### 3.3.2. Oxidation of LDPE surface accumulated $Pb^{2+}$ to $Pb^{4+}$

Free chlorine residuals are capable to oxidize $Pb^{2+}$ to $Pb^{4+}$ by forming $PbO_2$ precipitates in the aqueous solution and reduce the Pb accumulation onto the LDPE surface (; Zhang and Lin, 2011) the redox reaction of LDPE surface accumulated $Pb^{2+}$ to $Pb^{4+}$ due to the exposure to chlorine residuals is given below:

$$Pb^{2+} + HOCl + H_2O \rightarrow PbO_2 + HCl \quad E_H^0 = 2.94\,(V)$$

The additional XPS analysis was conducted to identify how exposure to free chlorine residuals alters the oxidation state of Pb ions deposited onto the LDPE surface. The Pb(4f) spectra for LDPE exposed to Pb only and Pb + free chlorine residuals are shown in Fig. 6. The doublet peak of Pb 4f spectra for LDPE exposed to the Pb in absence of free chlorine residuals were located at 137.6 and 143 eV binding energies, respectively, and suggested the presence of $Pb^{2+}$ in from of $Pb(OH)_2$ as predicted through precipitation reaction (Pederson, 1982). However, the shoulder peaks of Pb(4f) occurred in samples exposed to the free chlorine residuals. After decomposing its spectra through Gaussian-Lorentzian curve fitting, the binding energies of Pb(4f7/2 and 2f5/2) at 138.9 eV and 144.1 eV were associated with $Pb^{4+}$, and suggested oxidation of $Pb^{2+}$ to $Pb^{4+}$ through formation of $PbO_2$ (Murray, 1981; Pederson, 1982). This curve fitting revealed that 58 % of total Pb deposited onto the LDPE surface was oxidized to $Pb^{4+}$ due to the presence of free chlorine residual and the remaining 42 % was present as $Pb^{2+}$.

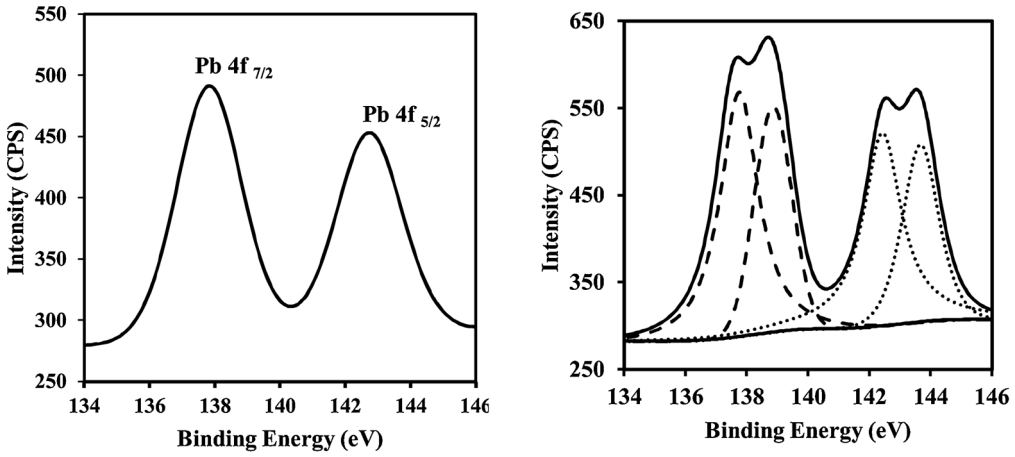


**Fig. 6.** X-ray photoelectron spectroscopy (XPS) spectra of Pb.

### 3.4. Investigate the factors influence Pb release from LDPE surface

The results showed the Pb release from LDPE surface into the synthetic water at pH 5.0 and 7.8 under dynamic condition during the 5-day release period (Fig. 7). This suggests gradual detachment of Pb species accumulated onto the LDPE surface into the water, which might be due to the shear forces applied during the dynamic mixing along with the concentration gradient toward the contact water. In response to the concentration gradient, diffusion of the Pb species from the LDPE surface into the contact water may occur and will continue until an equilibrium concentration is reached (). The greater level of Pb release into the contact water occurred by a reduction of the pH of contact water from 7.8 to 5.0. After 5 min exposure to the synthetic water at pH 5.0, approximately 65 % of $Pb^{2+}$ species were released however, only 4% were released at pH 7.8. This could be due to the greater solubility of precipitated $Pb^{2+}$ species at the lower pH levels (Kim et al., 2011; Lasheen et al., 2008). The study conducted by Turner and Holmes (2015) also reported a lower level of Pb species left in the aqueous solution at pH 8.0 (~15 %) compared to the pH 5.0 (~30 %) after conducting the microplastics metal exposure experiment (Santos-Echeandía et al., 2020). The literature investigated heavy metal release from plastic surface are limited. The recent study conducted by Fernández et al., (2020) demonstrated 37 % Hg released from virgin and non-aged micro plastics under dynamic flow condition in first 2 h contact with the sea water. This Hg release has been increased up to 12 % following 7 days exposure period (Fernández et al., 2020). However; in the present study, 73 % Pb was released after 2 h and approached to 86 % release after 5 days. Similar to our findings the metal species adsorbed onto immobile site of polymer surface have high stability constant which limits the rate of diffusion of Hg in the water. Moreover, as our speciation graph in Fig. 3 showed the primary forms of $Pb^{2+}$ in water are $Pb(OH)_2$ and $PbCO_3$ precipitates (67 % of $[Pb]_t$) at pH 7.8, however by pH reduction to 5.0, these precipitates accumulated on LDPE surface could be dissolved into the water and be converted to the $Pb^{2+}$ dissolved ions. At pH 5.0, a greater level of surface deposited Pb was released to the contact water under dynamic condition (86 % after 5 days) compared to the static condition (22 % after 5 days) (**Figure SI-7**).

The dynamic condition caused by stirring the LDPE pellets in synthetic water during the release experiments increased the percentage of Pb release, by accelerating the mass transfer of Pb out of the LDPE surface to the water (Xie and Giammar, 2011). Immobile water adjacent to the Pb accumulated LDPE surface was not well mixed with the bulk water; therefore, that declined the concentration gradient and might limit the Pb release under stagnant condition. The lower percentage of surface accumulated Pb species was released from aged LDPE pellets (9%) compared to the new LDPE pellets (65 %) after immediate exposure to synthetic water at pH 5.0 (Fig. 8). This might be due to Pb species stronger surface attachments and electrostatic association to the oxidized LDPE surface (Salehi et al., 2018b). This result agreed with Santos-Echeandía et al. (2020) findings which reported that highly degraded microplastics recovered from different beaches experienced a greater quantity of Hg deposition due to their anionic active surface

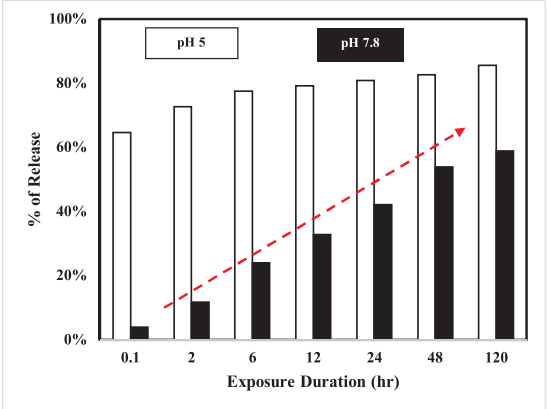


**Fig. 7.** Percentage of Pb release from new LDPE at pH 5.0 and 7.8 (dynamic condition).

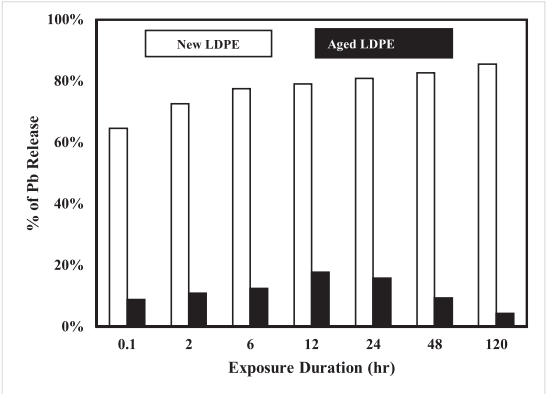


**Fig. 8.** Percentage of Pb release from new and aged LDPE surface at pH 5.0 (dynamic condition).

sites and surface chemistry alterations caused by photooxidation (Santos-Echeandía et al., 2020). Surprisingly, after a 24 h release period, instead of Pb releasing, some Pb species were absorbed onto the aged LDPE surface. This could be due to the electrostatic attraction of oxidized LDPE surface toward Pb species. However, initially, some of the adsorbed species were detached from the surface due to the concentration gradient and shear forces applied by stirring the solution, but they have resorbed onto the active surface sites over time.

### 3.5. Implication to the potable water plumbing pipes

Exposure to lead-contaminated tap water remains a serious public health concern nationally and globally. Plastic plumbing materials are increasingly being used to rehabilitate aging water infrastructure and construct new potable water systems as well as to limit cost and avoid drinking water quality and safety concerns associated with metal pipe corrosion. It is expected that replacing the corroded lead pipes with the plastic pipes will prevent lead exposure. However, other lead-bearing plumbing materials like brass valves and fittings, galvanized iron, lead-tin solders, and faucets could release lead into the water conveyed by the plastic plumbing. This study demonstrated that biofilm accumulation onto the plastic surface promotes the lead uptake. This finding along with the previous literature that indicated a greater biofilm accumulation onto the plastic plumbing than copper pipes raising concerns regarding an enhanced potential risk of plastic pipes toward the public safety compared to the copper pipes (Lehtola et al., 2004; Taylor et al., 2009; Liu et al., 2017). The variation of lead deposition onto and release from the plastic surface by water chemistry conditions highlights the role of water sources, treatment practices, and water quality fluctuations on lead mobility within the building plumbing systems. Furthermore, the greater number of available surface sites provided by the aged plastics for lead accumulation, underscores the importance of plastic pipes stability. This informs the plastic pipes' manufacturers to generate more thermo-oxidative resistance pipes to suppress the risk of lead accumulation within the plumbing while improving the pipes service life. This research revealed the significant role of chlorine residuals on reduced lead deposition onto the plastic pipes by forming the $PbO_2$(s) precipitates and inhibiting the biofilm development onto the pipe surface. Thus, the water distribution systems could reduce the degree of lead deposition onto the building plumbing by maintaining the proper level of disinfectant residuals. Lead deposition onto plastic pipes could become a public health threat, when these deposits are released into tap water. It was found that water chemistry fluctuations like pH reduction and chlorine concentration could result in Pb release from the plastic surface back to the drinking water. Thus, the water utilities using blending or differently source water should develop strategies to avoid the significant water pH fluctuations within their network to limit the risk of metal release to the people's tap water The Pb release pattern from the plastic surface could vary depending on the degree of plastic surface oxidation under static and dynamic conditions. These results are applicable in the new and aged polyethylene pipes used for the drinking water plumbing.

## 4. Conclusion

In this study, the influence of biofilm presence, water chemistry conditions, and chlorine residuals on $Pb^{2+}$ deposition onto the LDPE surface was investigated. Two novel approaches have been developed to quantify the biofilm accumulated onto the LDPE surface and examine the interrelation between biofilm biomass and $Pb^{2+}$ accumulation. In addition, the effect of water pH on $Pb^{2+}$ release from LDPE surface was investigated under static and dynamic conditions. A more significant Pb surface loading was found on LDPE with biofilm (1602 $\mu g/m^2$) compare to LDPE with no biofilm (124 $\mu g/m^2$). The biofilm accumulation on the LDPE surface enhanced the surface sites available for $Pb^{2+}$ adsorption and increased its uptake. The Pseudo 2nd order kinetic model was fitted into the experimental $Pb^{2+}$ adsorption data for the LDPE surface with the biofilm. The greater ionic strength and competitive ions presence in aqueous solution significantly reduced Pb accumulation onto the LDPE surface. The presence of chlorine residuals in the aqueous solution resulted in the lower Pb uptake by the LDPE surface. The XPS spectroscopy confirmed oxidation of surface deposited $Pb^{2+}$ to $Pb^{4+}$ due to the exposure to free chlorine residuals. A higher level of Pb was released from the LDPE surface into the water under dynamic conditions compared to the static tests. A lower water pH increased the Pb release into the contact water under dynamic condition.

## CRediT authorship contribution statement

**Tanvir Ahamed:** Investigation, Writing - original draft, Visualization. **Shawn P. Brown:** Methodology. **Maryam Salehi:** Conceptualization, Methodology, Validation, Supervision.

## Declaration of Competing Interest

The authors declare that they have no known competing financial interests or personal relationships that could have appeared to influence the work reported in this paper.

## Acknowledgments

The authors thank Dr. Gary Bowlin and Benjamin Minden at the University of Memphis, Biomedical Engineering Department, for their assistance in using the fluorescence microscope and hemocytometer. The authors appreciate Dr. Paul Simone and Dr. Gary Emmert at the Chemistry Department for their assistance with the metal's quantifications. Additional thanks to Donya Sharafoddinzadeh in Civil Engineering Department for her help in Atomic Absorption machine utilization. Special thanks to Dr. Felio Perez (Materials Science Lab Manager, The University of Memphis) for assisting in X-ray photoelectron spectroscopy (XPS) analysis.

## Appendix A. Supplementary data

Supplementary material related to this article can be found, in the online version, at doi:https://doi.org/10.1016/j.jhazmat.2020.123253.

## References

Boudrahem, F., Aissani-Benissad, F., Soualah, A., 2011. Adsorption of lead(II) from aqueous solution by using leaves of date trees as an adsorbent. J. Chem. Eng. Data 56 (5), 1804–1812. https://doi.org/10.1021/je100770j.

Boyd, G.R., Pierson, G.L., Kirmeyer, G.J., English, R.J., 2008. Lead variability testing in seattle public schools. J. Am. Water Work Assoc. 100 (2), 53–64.

Council on Environmental Health, 2016. Prevention of Childhood Lead Toxicity. In Pediatrics; American Association of Pediatrics: Itasca. IL, USA.

DeSimone, D., Sharafoddinzadeh, D., Salehi, M., 2020. "Prediction of Children's Blood Lead Levels from Exposure to Lead in Schools' Drinking Water ? A Case Study in Tennessee, USA". Water Journal, Special Issue of Water Quality in Buildings 12 (6), 1826.

Edwards, M., Triantafyllidou, S., Best, D., 2009. Elevated blood lead in young children due to lead-contaminated drinking water: washington, DC, 2001 – 2004. Environ. Sci. Technol. 43 (5), 1618–1623.

Elfland, C., Paolo, S., Marc, E., 2010. Lead-contaminated water from brass plumbing devices in new buildings. J. Am. Water Work Assoc. 102 (11), 66–76.

Feder, M., Phoenix, V., Haig, S., Sloan, W., Dorea, C., Haynes, H., 2015. Influence of biofilms on heavy metal immobilization in sustainable urban drainage systems (SuDS). Environ. Technol. (UK) 36 (21), 2803–2814. https://doi.org/10.1080/09593330.2015.1049214.

Fein, J.B., Daughney, C.J., Yee, N., Davis, T.A., 1997. A chemical equilibrium model for metal adsorption onto bacterial surfaces. Geochim. Cosmochim. Acta. 61 (16), 3319–3328. https://doi.org/10.1016/S0016-7037(97)00166-X.

Fernández, B., Santos-Echeandía, J., Rivera-Hernández, J.R., Garrido, S., Albentosa, M., 2020. Mercury interactions with algal and plastic microparticles: comparative role as vectors of metals for the mussel, Mytilus galloprovincialis. J. Hazard. Mater. 396, 122739. https://doi.org/10.1016/j.jhazmat.2020.122739.

Fish, K.E., Collins, R., Green, N.H., et al., 2015. Characterisation of the physical composition and microbial community structure of biofilms within a model full-scale

drinking water distribution system. PLoS One 10 (2), 1–22. https://doi.org/10.1371/journal.pone.0115824.
González-Rivas, F., Ripolles-Avila, C., Fontecha-Umaña, F., Ríos-Castillo, A.G., Rodríguez-Jerez, J.J., 2018. Biofilms in the spotlight: detection, quantification, and removal methods. Compr. Rev. Food Sci. Food Saf. 17 (5), 1261–1276. https://doi.org/10.1111/1541-4337.12378.
Ho, Y.S., McKay, G., 1999. Pseudo-second order model for sorption processes. Process Biochem. 34 (5), 451–465. https://doi.org/10.1016/S0032-9592(98)00112-5.
Holmes, L., Turner, A., Thompson, R.C., 2014. Interactions between trace metals and plastic production pellets under estuarine conditions. Mar. Chem. 167, 25–32. https://doi.org/10.1016/j.marchem.2014.06.001.
Huang, X., Zhao, S., Abu-Omar, M., Whelton, A.J., 2017. In-situ cleaning of heavy metal contaminated plastic water pipes using a biomass derived ligand. J. Environ. Chem. Eng. 5 (4), 3622–3631. https://doi.org/10.1016/j.jece.2017.07.003.
Huang, X., Zemlyanov, D.Y., Diaz-Amaya, S., Salehi, M., Stanciu, L., Whelton, A., 2019a. Competitive heavy metal adsorption onto new and aged polyethylene under various drinking water conditions. J. Hazard. Mater.
Huang, Xiangning, Zemlyanov, Dmitry Y., Diaz-Amaya, Susana, Salehi, Maryam, Lia Stanciu, A.J.W., 2019b. Competitive heavy metal adsorption onto new and aged polyethylene under various drinking water conditions. J. Hazard. Mater Accepted.
Huang, Xiangning, Zemlyanov, Dmitry Y., Diaz-Amaya, Susana, Salehi, Maryam, Lia Stanciu, A.J.W., 2019c. Competitive heavy metal adsorption onto new and aged polyethylene under various drinking water conditions. J. Hazard. Mater. (November 2019), 121585. https://doi.org/10.1016/j.jhazmat.2019.121585. Accepted.
Huang, X., Pieper, K.J., Cooper, H.K., Diaz-Amaya, S., Zemlyanov, D.Y., Whelton, A.J., 2019d. Corrosion of upstream metal plumbing components impact downstream PEX pipe surface deposits and degradation. Chemosphere 236, 124329. https://doi.org/10.1016/j.chemosphere.2019.07.060.
Inglezakis, V.J., Zorpas, A.A., Loizidou, M.D., Grigoropoulou, H.P., 2005. The effect of competitive cations and anions on ion exchange of heavy metals. Sep. Purif. Technol. 46 (3), 202–207. https://doi.org/10.1016/j.seppur.2005.05.008.
Jain, N.B., Laden, F., Guller, U., Shankar, A., Kasani, S., Garshick, E., 2005. Relation between blood lead levels and childhood anemia in India. Am. J. Epidemiol. 161 (10), 968–973. https://doi.org/10.1093/aje/kwi126.
Javanbakht, V., Zilouei, H., Karimi, K., 2011. Lead biosorption by different morphologies of fungus Mucor indicus. Int. Biodeterior. Biodegrad. 65 (2), 294–300. https://doi.org/10.1016/j.ibiod.2010.11.015.
Kelley, K.M., Stenson, A.C., Dey, R., Whelton, A.J., 2014. Release of drinking water contaminants and odor impacts caused by green building cross-linked polyethylene (PEX) plumbing systems. Water Res. 67, 19–32. https://doi.org/10.1016/j.watres.2014.08.051.
Kim, E.J., Herrera, J.E., Huggins, D., Braam, J., Koshowski, S., 2011. Effect of pH on the concentrations of lead and trace contaminants in drinking water: a combined batch, pipe loop and sentinel home study. Water Res 45 (9), 2763–2774. https://doi.org/10.1016/j.watres.2011.02.023.
Lasheen, M.R., Sharaby, C.M., El-Kholy, N.G., Elsherif, I.Y., El-Wakeel, S.T., 2008. Factors influencing lead and iron release from some Egyptian drinking water pipes. J. Hazard. Mater. 160 (2–3), 675–680. https://doi.org/10.1016/j.jhazmat.2008.03.040.
LEED for Homes Rating System, 2008. LEED for Homes Rating System. US Green Build Counc.
Lehtola, M.J., Miettinen, I.T., Keinänen, M.M., et al., 2004. Microbiology, chemistry and biofilm development in a pilot drinking water distribution system with copper and plastic pipes. Water Res. 38 (17), 3769–3779. https://doi.org/10.1016/j.watres.2004.06.024.
Lehtola, M.J., Laxander, M., Miettinen, I.T., Hirvonen, A., Vartiainen, T., Martikainen, P.J., 2006. The effects of changing water flow velocity on the formation of biofilms and water quality in pilot distribution system consisting of copper or polyethylene pipes. Water Res. 40 (11), 2151–2160.
Lewandowski, Z., Webb, D., Hamilton, M., 1999. Harkin G. Quantifying biofilm structure. Water Sci. Technol. 39 (7), 71–76. https://doi.org/10.1016/S0273-1223(99)00152-3.
Liu, H., Korshin, G.V., Ferguson, J.F., 2009. Interactions of Pb (II)/Pb (IV) solid phases with chlorine and their effects on lead release. Environ. Sci. Technol. 43 (9), 3278–3284.
Liu, W., Wang, T., Borthwick, A.G.L., et al., 2013. Adsorption of Pb2+, Cd2+, Cu2+ and Cr3+ onto titanate nanotubes: competition and effect of inorganic ions. Sci. Total Environ. 456–457, 171–180. https://doi.org/10.1016/j.scitotenv.2013.03.082.
Liu, G., Tao, Y., Zhang, Y., et al., 2017. Hotspots for selected metal elements and microbes accumulation and the corresponding water quality deterioration potential in an unchlorinated drinking water distribution system. Water Res. 124, 435–445. https://doi.org/10.1016/j.watres.2017.08.002.
Marsili, E., Kjelleberg, S., Rice, S.A., 2018. Mixed Community Biofilms and Microbially Influenced Corrosion. pp. 2–7. https://doi.org/10.1080/154281196. 1982.
Masters, S., Welter, G.J., Edwards, M., 2016. Seasonal variations in lead release to potable water. Environ. Sci. Technol. 50 (10), 5269–5277. https://doi.org/10.1021/acs.est.5b05060.
Muhammad, N., Parr, J., Smith, M.D., Wheatley, A.D., 1998. Microbial uptake of heavy metals in slow sand filters. Environ. Technol. (UK) 19 (6), 633–638. https://doi.org/10.1080/09593331908616720.
Munier, B., Bendell, L.I., 2018. Macro and micro plastics sorb and desorb metals and act as a point source of trace metals to coastal ecosystems. PLoS One 13 (2), 1–13. https://doi.org/10.1371/journal.pone.0191759.
Murray, J.W., 1981. X-ray photoelectron spectroscopic (XPS) studies on the chemical nature of metal ions adsorbed on clays and minerals. Adsorpt From Aqueous Solut (January). https://doi.org/10.1007/978-1-4613-3264-0.
Niquette, P., Servais, P., Savoir, R., 2000. Impacts of pipe materials on densities of fixed bacterial biomass in a drinking water distribution system. Water Res. 34 (6), 1952–1956. https://doi.org/10.1016/S0043-1354(99)00307-3.
Ohsumi, T., Takenaka, S., Wakamatsu, R., et al., 2015. Residual structure of Streptococcus mutans biofilm following complete disinfection favors secondary bacterial adhesion and biofilm Re-development. PLoS One 10 (1), 1–12. https://doi.org/10.1371/journal.pone.0116647.
Olson, T.M., Wax, M., Yonts, J., et al., 2017. Forensic estimates of lead release from lead service lines during the Water Crisis in Flint, Michigan. Environ. Sci. Technol. Lett. 4 (9), 356–361. https://doi.org/10.1021/acs.estlett.7b00226.
Olu-Owolabi, B.I., Diagboya, P.N., Ebaddan, W.C., 2012. Mechanism of Pb2+ removal from aqueous solution using a nonliving moss biomass. Chem. Eng. J. 195–196, 270–275. https://doi.org/10.1016/j.cej.2012.05.004.
Pederson, L.R., 1982. Two-dimensional chemical-state plot for lead using XPS. J. Electron Spectros. Relat. Phenomena 28 (2), 203–209. https://doi.org/10.1016/0368-2048(82)85043-3.
Peng, C.Y., Hill, A.S., Friedman, M.J., et al., 2012. Occurrence of trace inorganic contaminants in drinking water distribution systems. J. Am. Water Works Assoc. 104 (3), 53–54. https://doi.org/10.5942/jawwa.2012.104.0042.
Powell, B.J.C., West, J.R., Hallam, N.B., Forster, C.F., 2000a. Performance of various kinetic models for chlorine decay. Water Resour 126 (February), 13–20. https://doi.org/10.1061/(ASCE)0733-9496(2000)126:1(13).
Powell, J.C., Hallam, N.B., West, J.R., Forster, C.F., Simms, J., 2000b. Factors which control bulk chlorine decay rates. Water Res. 34 (1), 117–126.
Priester, J.H., Horst, A.M., Van De Werfhorst, L.C., Saleta, J.L., Mertes, L.A.K., Holden, P.A., 2007. Enhanced Visualization of Microbial Biofilms by Staining and Environmental Scanning Electron Microscopy. J. Microbiol. Methods 68 (3), 577–587. https://doi.org/10.1016/j.mimet.2006.10.018.
Proctor, C.R., Rhoads, W.J., Keane, T., Salehi, M., Hamilton, K., Pieper, K.J., Cwiertny, D.M., Prevost, M., Whelton, A.J., 2020. “Considerations for large building water quality after extended stagnation”. Journal of American Water Works Association Water Science. https://doi.org/10.1002/aws2.1186. Accepted Manuscript.
Rajasekharan, V.V., Clark, B.N., Boonsalee, S., Switzer, J.A., 2007. Electrochemistry of free chlorine and monochloramine and its relevance to the presence of Pb in drinking water. Environ. Sci. Technol. 41 (12), 4252–4257. https://doi.org/10.1021/es062922t.
Rhoads, W.J., Pruden, A., Edwards, M.A., 2017. Interactive effects of corrosion, copper, and chloramines on Legionella and mycobacteria in hot water plumbing. Environ. Sci. Technol. 51 (12), 7065–7075. https://doi.org/10.1021/acs.est.6b05616.
Richter-Heitmann, T., Eickhorst, T., Knauth, S., Friedrich, M.W., Schmidt, H., 2016. Evaluation of strategies to separate root-associated microbial communities: a crucial choice in rhizobiome research. Front. Microbiol. 7, 1–11. https://doi.org/10.3389/fmicb.2016.00773.
Rożej, A., Cydzik-Kwiatkowska, A., Kowalska, B., Kowalski, D., 2015. Structure and microbial diversity of biofilms on different pipe materials of a model drinking water distribution systems. World J. Microbiol. Biotechnol. 31 (1), 37–47. https://doi.org/10.1007/s11274-014-1761-6.
Rummel, C.D., Jahnke, A., Gorokhova, E., Kühnel, D., Schmitt-Jansen, M., 2017. Impacts of biofilm formation on the fate and potential effects of microplastic in the aquatic environment. Environ. Sci. Technol. Lett. 4 (7), 258–267. https://doi.org/10.1021/acs.estlett.7b00164.
Salehi, M., Johari, M.S., 2011. Study of Fiber packing density of lyocell ring-spun yarns. J. Text Inst 102 (5), 389–394. https://doi.org/10.1080/00405000.2010.482341.
Salehi, M., Li, X., Whelton, A.J., 2017. Metal accumulation in representative plastic drinking water plumbing systems. J. Am. Water Works Assoc. 109 (11), E479–E493. https://doi.org/10.5942/jawwa.2017.109.0117.
Salehi, M., Abouali, M., Wang, M., et al., 2018a. Case study: fixture water use and drinking water quality in a new residential green building. Chemosphere 195, 80–89.
Salehi, M., Jafvert, C.T., Howarter, J.A., Whelton, A.J., 2018b. Investigation of the factors that influence lead accumulation onto polyethylene : implication for potable water plumbing pipes. J. Hazard. Mater. 347, 242–251.
Salehi, M., Odimayomi, T., Ra, K., et al., 2019. An investigation of spatial and temporal drinking water quality variation in green residential plumbing. J. Build Environ (xxxx).
Santos-Echeandía, J., Rivera-Hernández, J.R., Rodrigues, J.P., Moltó, V., 2020. Interaction of mercury with beached plastics with special attention to zonation, degradation status and polymer type. Mar. Chem. 222 (October 2019), 103788. https://doi.org/10.1016/j.marchem.2020.103788.
Shakhsi-Niaei, M., Salehi Esfandarani, M., 2019. Multi-objective deterministic and robust models for selecting optimal pipe materials in water distribution system planning under cost, health, and environmental perspectives. J. Clean. Prod. 207, 951–960. https://doi.org/10.1016/j.jclepro.2018.10.071.
Stewart, B.R., 2005. Corrosion resistance, ease of installation stimulate demand for plastic pipe. Plast Eng 14–22.
Subramanian, K.S., Sastri, V.S., Elboujdaini, M., Connor, J.W., Davey, A.B.C., 1995. Water contamination: impact of tin-lead solder. Water Res. 29 (8), 1827–1836. https://doi.org/10.1016/0043-1354(95)00005-6.
Suguna, M., Siva Kumar, N., 2013. Equilibrium, Kinetic and Thermodynamic Studies on Biosorption of Lead(II) and Cadmium(II) from Aqueous Solution by Polypores Biomass. Indian J. Chem. Technol 20 (1), 57–69.
Switzer, J.A., Rajasekharan, V.V., Boonsalee, S., Kulp, E.A., Bohannan, E.W., 2006. Evidence that monochloramine disinfectant could lead to elevated Pb levels in drinking water. Environ. Sci. Technol. 40 (10), 3384–3387. https://doi.org/10.1021/es052411r.
Taylor, P., Percival, S.L., Walker, J.T., 2009. Potable Water and Biofilms : a Review of the Public Health Implications. Biofouling: J. Bioad. Biofilm. Res. (May 2014), 37–41.

https://doi.org/10.1080/08927019909378402.
Turner, A., Holmes, L.A., 2015. Adsorption of trace metals by microplastic pellets in fresh water. Environ. Chem. 12 (5), 600–610. https://doi.org/10.1071/EN14143.
Unuabonah, E.I., Adebowale, K.O., Olu-Owolabi, B.I., Yang, L.Z., Kong, L.X., 2008. Adsorption of Pb (II) and Cd (II) from aqueous solutions onto sodium tetraborate-modified kaolinite clay: equilibrium and thermodynamic studies. Hydrometallurgy 93 (1–2), 1–9. https://doi.org/10.1016/j.hydromet.2008.02.009.
Vargas, I.T., Alsina, M.A., Pavissich, J.P., et al., 2014. Multi-technique approach to assess the effects of microbial biofilms involved in copper plumbing corrosion. Bioelectrochemistry 97, 15–22. https://doi.org/10.1016/j.bioelechem.2013.11.005.
Vasquez, F.A., Heaviside, R., Tang, Z., Taylor, J.S., 2006. Effect of free chlorine and chloramines on lead release in a distribution system. J. Am. Water Work Assoc. 98 (2). https://doi.org/10.1017/CBO9781107415324.004.
Vilar, V.J.P., Botelho, C.M.S., Boaventura, R.A.R., 2007. Kinetics and equilibrium modelling of lead uptake by algae Gelidium and algal waste from agar extraction industry. J. Hazard. Mater. 143 (1–2), 396–408. https://doi.org/10.1016/j.jhazmat.2006.09.046.
Wang, Y.I.N., Xie, Y., Li, W., Wang, Z., Giammar, D.E., 2010. Formation of lead (IV) oxides from lead (II) compounds. Environ. Sci. Technol. 44 (23), 8950–8956.
Whelton, A.J., Nguyen, T., 2013. Contaminant migration from polymeric pipes used in buried potable water distribution systems: a review. Crit. Rev. Environ. Sci. Technol. 43 (7), 679–751. https://doi.org/10.1080/10643389.2011.627005.
Wu, X.L., Zhao, D., Yang, S.T., 2011. Impact of solution chemistry conditions on the sorption behavior of Cu(II) on Lin'an montmorillonite. Desalination 269 (1–3), 84–91. https://doi.org/10.1016/j.desal.2010.10.046.
Xie, Y., 2010. Dissolution, Formation, and Transformation of the Lead Corrosion Product PbO 2 : Rates and Mechanisms of Reactions that Control Lead Release in Drinking Water Distribution Systems. Diss. Washingt. Univ. Open Scholarsh(January). https://doi.org/10.1177/1073191116659740.
Xie, Y., Giammar, D.E., 2011. Effects of flow and water chemistry on lead release rates from pipe scales. Water Res. 45 (19), 6525–6534. https://doi.org/10.1016/j.watres.2011.09.050.
Yang, E., Faust, K.M., 2019. Dynamic public perceptions of water infrastructure in US shrinking cities: end-user trust in providers and views toward participatory processes. J. Water Resour Plan Manag. 145 (9), 1–13. https://doi.org/10.1061/(ASCE)WR.1943-5452.0001093.
Yang, X., Beyenal, H., Harkin, G., 2000. Lewandowski Z. Quantifying biofilm structure using image analysis. J. Microbiol. Methods 39 (2), 109–119. https://doi.org/10.1016/S0167-7012(99)00097-4.
Yee, N., Fein, J.B., 2002. Does metal adsorption onto bacterial surfaces inhibit or enhance aqueous metal transport? Column and batch reactor experiments on Cd-Bacillus subtilis-quartz systems. Chem. Geol. 185 (3–4), 303–319. https://doi.org/10.1016/S0009-2541(01)00412-0.
Zhang, Y., Edwards, M., 2011. Effects of pH, chloride, bicarbonate, and phosphate on brass dezincification. J. Am. Water Works Assoc. 103 (4), 90–102.
Zhang, Y., Lin, Y.P., 2011. Determination of PbO2 formation kinetics from the chlorination of Pb(II) carbonate solids via direct PbO2 measurement. Environ. Sci. Technol. 45 (6), 2338–2344. https://doi.org/10.1021/es1039826.
Zhang, C., Li, C., Zheng, X., Zhao, J., He, G., Zhang, T., 2017. Effect of pipe materials on chlorine decay, trihalomethanes formation, and bacterial communities in pilot-scale water distribution systems. Int. J. Environ. Sci. Technol. (Tehran) 14 (1), 85–94. https://doi.org/10.1007/s13762-016-1104-2.